

Published in final edited form as:

*Nat Plants*. 2018 August ; 4(8): 548–553. doi:10.1038/s41477-018-0204-z.

## Maternal auxin supply contributes to early embryo patterning in *Arabidopsis*

Hélène S. Robert<sup>#1,2,\*</sup>, Chulmin Park<sup>#3,‡</sup>, Carla Loreto Guitérrez<sup>#3</sup>, Barbara Wójcikowska<sup>1,4</sup>, Aleš P n ík<sup>5</sup>, Ond ej Novák<sup>5</sup>, Junyi Chen<sup>6</sup>, Wim Grunewald<sup>2</sup>, Thomas Dresselhaus<sup>6</sup>, Ji í Friml<sup>7,\*</sup>, and Thomas Laux<sup>3,\*</sup>

<sup>1</sup>Mendel Centre for Genomics and Proteomics of Plants Systems, CEITEC MU - Central European Institute of Technology, Masaryk University, 625 00 Brno, Czech Republic <sup>2</sup>Department of Plant Systems Biology, Flanders Institute for Biotechnology (VIB) and Department of Plant Biotechnology and Bioinformatics, Ghent University, 9052 Gent, Belgium <sup>3</sup>BIOSS Centre for Biological Signaling Studies, Faculty of Biology, Albert-Ludwigs-Universität Freiburg, 79104 Freiburg, Germany <sup>4</sup>Department of Genetics, Faculty of Biology and Environmental Protection, University of Silesia, 40-032 Katowice, Poland <sup>5</sup>Laboratory of Growth Regulators, Centre of the Region Haná for Biotechnological and Agricultural Research, Faculty of Science of Palacký University & Institute of Experimental Botany CAS, 783 71 Olomouc, Czech Republic <sup>6</sup>Cell Biology and Plant Biochemistry, Biochemie-Zentrum Regensburg, University of Regensburg, 93053 Regensburg, Germany <sup>7</sup>Institute of Science and Technology Austria (IST Austria), 3400 Klosterneuburg, Austria

# These authors contributed equally to this work.

### Introductory paragraph

The angiosperm seed is composed of three genetically distinct tissues: the diploid embryo that originates from the fertilized egg cell, the triploid endosperm that is produced from the fertilized central cell, and the maternal sporophytic integuments that develop into the seed coat<sup>1</sup>. At the onset of embryo development in *Arabidopsis thaliana*, the zygote divides asymmetrically

Users may view, print, copy, and download text and data-mine the content in such documents, for the purposes of academic research, subject always to the full Conditions of use:[http://www.nature.com/authors/editorial\\_policies/license.html#terms](http://www.nature.com/authors/editorial_policies/license.html#terms)

Correspondence and requests for material should be sent to Hélène S. Robert ([helene.robert.boisivon@ceitec.muni.cz](mailto:helene.robert.boisivon@ceitec.muni.cz)), Jiri Friml ([jiri.friml@ist.ac.at](mailto:jiri.friml@ist.ac.at)), Thomas Laux ([laux@biologie.uni-freiburg.de](mailto:laux@biologie.uni-freiburg.de)).

\*Current address: Gregor Mendel Institute of Molecular Plant Biology, Austrian Academy of Sciences, 1030 Vienna, Austria.

#### Data availability

The data that supports the findings of this study are available from the corresponding authors upon request.

#### Accession numbers

*ABC1/PGPI* (At2g36910), *ABC19/PGPI9* (At3g28860), *AUX1* (At2g38120), *BAN* (At1g61720), *BDL/IAA12* (At1g04550), *LAX1* (At5g01240), *PIN3* (At1g70940), *R2D2* (NASC ID N2105637), *TAA1* (At1g70560), *TAR1* (At4g24670), *YUC1* (At4g32540), *YUC4* (At5g11320), *YUC8* (At4g28720), *YUC9* (At1g04180), *WOX2* (At5g59340), *p35S:DII-VENUS* (NASC ID 799173), *p35S:mDII-VENUS* (NASC ID 799174).

#### Author contributions

H.S.R., C.P. and C.L.G. contributed equally to this work, performed experiments. H.S.R., B.W., A.P. and O.N. collected samples and performed the analysis for the auxin measurements. W.G. participated in the backcrosses experiments. J.C. and T.D. provided the maize data. H.S.R., C.P., C.L.G., J.F., and T.L. designed the experiments, analysed the data, and wrote the paper.

#### Competing interest

The authors declare no competing interest.

producing a small apical embryonic cell, and a larger basal cell that connects the embryo to the maternal tissue<sup>2</sup>. The coordinated and synchronous development of the embryo and the surrounding integuments, and the alignment of their growth axes suggest communication between maternal tissues and the embryo. In contrast to animals, however, where a network of maternal factors that direct embryo patterning have been identified<sup>3,4</sup>, only a few maternal mutations have been described to affect embryo development in plants<sup>5–7</sup>. Early embryo patterning in *Arabidopsis* requires accumulation of the phytohormone auxin in the apical cell by directed transport from the suspensor<sup>8–10</sup>. However, the origin of this auxin has remained obscure. Here we investigate the source of auxin for early embryogenesis and provide evidence that the mother plant coordinates seed development by supplying auxin to the early embryo from the integuments of the ovule. We show that auxin response increases in ovules upon fertilization, due to upregulated auxin biosynthesis in the integuments, and this maternally-produced auxin is required for correct embryo development.

## Keywords

*Arabidopsis thaliana*; maize; auxin; auxin biosynthesis; embryogenesis; maternal sporophytic effect

---

The different developmental perspectives of the two daughter cells (Fig. 1a) of the *Arabidopsis* zygote are controlled by several factors. Among them, polarized auxin flow from the basal daughter cell via the PIN7 auxin transporter leads to auxin accumulation and activation of downstream responses in the apical daughter cell, which ultimately contributes to its specification as the founder of the proembryo<sup>9,10</sup>.

In search for the source of the auxin mediating early embryo development<sup>9</sup>, we measured free auxin and auxin derivatives in *Arabidopsis* ovules. We found that the levels of active auxin (IAA) and of the catabolic intermediates IAA-Aspartate (IAAsp) and oxidized IAA (oxIAA) strongly increase 24 h after pollination (24 HAP; Fig. 1b and Supplementary Table 1). At this stage, fertilization has usually occurred, as judged by the appearance of endosperm nuclei (not shown). To localize auxin accumulation in the ovule, we used the *p35S*-driven DII-VENUS auxin signaling sensor that rapidly degrades in response to auxin, and therefore negatively monitors relative cellular auxin levels<sup>11</sup>. 24 HAP, DII-VENUS signals become strongly reduced throughout the ovule compared to 0 HAP, indicating an increased amount of auxin (Fig. 1c-d). Control experiments confirm that sensor degradation was measured (Supplementary Fig. 1 and Supplementary Table 2). We quantified the DII signal using the R2D2 reporter that combines an *pRPS5A*-driven DII-VENUS with an *pRPS5A*-driven auxin-insensitive mDII-tdTomato as internal reference<sup>12</sup>. The mDII/DII signal ratio provides a quantitative measure of the cellular auxin signal. mDII/DII initially decreases before pollination (compare 0 HAE, h after emasculation, and 0 HAP), and then increases again after pollination (24 HAP) (Fig. 1e and Supplementary Fig. 2a).

Auxin mediates the degradation of Aux/IAA transcriptional repressors, resulting in transcriptional auxin output<sup>13</sup>, which we monitored with the *pDR5:GFP* reporter<sup>9</sup>. We observed three localized *pDR5:GFP* maxima at 24 HAP: (1) in the integument region where the embryo attaches, (2) at the opposite chalazal side of the embryo sac, and (3) in the

funiculus that connects the ovule to the placenta (Fig. 1h and Supplementary Fig. 2b). By contrast, *pDR5:GFP* signal is weak or undetectable before pollination or in unpollinated controls (Fig. 1g and Supplementary Fig. 2b). Quantification in the embryo attachment region (outlined in Fig. 1a and Supplementary Fig. 2b) revealed that *pDR5:GFP* signal increases about 7 fold after pollination (Fig. 1e). We confirmed the observed changes of DII and *pDR5:GFP* expression in self-pollinated flowers, excluding that the upregulation was caused by emasculation or hand-pollination (Fig. 1f). Collectively, these results indicate that pollination leads to increased auxin levels in the maternal tissues surrounding the embryo and a localized upregulation of auxin response in the embryo attachment region.

To address whether upregulation of auxin response in the ovule by pollination is evolutionary conserved, we studied *pDR5:GFP* expression dynamics in the monocotyledonous maize. Unlike in *Arabidopsis*, the embryo sac in maize is entirely surrounded by several layers of nucellar tissue and thus is not in direct proximity to the integuments in the micropylar region. We find that *pDR5* expression is strongly upregulated by pollination in the tips of the integuments and in the nucellus cells at the micropylar region (Supplementary Fig. 3). Thus, despite their different ovule organization, we observed a similar increase of auxin response in maternal tissues in *Arabidopsis* and maize.

In *Arabidopsis*, auxin production via the indole-3-pyruvic acid (IPyA) pathway<sup>14</sup> is the main biosynthetic pathway and is catalyzed by the TRYPTOPHAN AMINOTRANSFERASE OF *ARABIDOPSIS* (TAA1) and related (TAR1 and TAR2) aminotransferases and by YUCCA (YUC) flavin monooxygenases<sup>15–17</sup>. Before pollination (0 HAP), we detected expression of a functional *pTAA1:GFP-TAA1* reporter in the embryo attachment region, in the chalaza, and funiculus (Fig. 1i, Supplementary Fig. 2c). Notably, *TAA1* expression is increased 24 HAP compared to 0 HAP in the embryo attachment region, whereas it is reduced in chalaza and funiculus (Fig. 1e,j and Supplementary Fig. 2c). *TAA1* expression in the embryo attachment region is also increased in self-pollinated flowers at 1 DAF (Days After Flowering) compared to FD (Flowering Day) (Fig. 1f), again confirming that the observed upregulation is not caused by hand-pollination. Unlike auxin response, however, *TAA1* expression increases with and without pollination to similar levels (compare UNP, unpollinated, and 24 HAP in Fig. 1e and Supplementary Fig. 2c). In addition, several *YUC* reporter genes are also expressed in the integuments (Supplementary Fig. 4 and Supplementary Table 2), of which *YUC8* and *YUC9* reporters appear upregulated at 16 HAP. In summary, the expression of the auxin biosynthetic machinery and the auxin signal output are differentially regulated during ovule maturation and pollination.

To address, whether upregulation of auxin biosynthesis is responsible for the elevated auxin response in the integuments, we studied auxin biosynthesis mutants. Profiling auxin metabolites revealed a strong reduction of IAA levels and its degradation products at 24 HAP in *wei8* (*weak ethylene insensitive8*, a recessive allele of *TAA1*) *tar1* ovules compared to wild type (Fig. 1b and Supplementary Table 1). Furthermore, *pDR5* reporter expression remains undetectable in the embryo attachment region at 24 HAP, and is reduced at chalaza and funiculus of *wei8* and more strongly in *wei8 tar1* auxin biosynthetic mutants, compared to wild type (Fig. 2a-d and Supplementary Table 2). Collectively, these data indicate that an

increased activity of the IPyA pathway is a major contributor of auxin accumulation in the integuments after pollination.

We then addressed the possible role of auxin production in the integuments for embryo development. Compared to wild type, embryos from selfed homozygous *wei8-1* mother plants display abnormal cell division patterns and suspensor exhibit aberrant cell divisions and reduced length at 2-cell to 8-cell embryo stages (Figs 2e, 3a and Supplementary Fig. 5). The earliest observed phenotypic abnormality is a horizontal division of the embryo apical daughter cells instead of the regular vertical one (arrows in Fig. 2e, Supplementary Fig. 5), suggesting that initial steps in apical-basal embryo development are compromised in *wei8* embryos. We observed similar defects in two independent alleles *wei8-3* and *wei8-11* (Figs 2e and 3b), confirming that they are caused by mutations in the *TAA1* gene. Because the frequencies of defective embryos are increased in *wei8 tar1* double mutants (Fig. 3a), we focused on *wei8 tar1* embryos for further analysis.

Because *TAA1* expression is undetectable in the embryo before the 16-cell stage<sup>10,18</sup>, we hypothesized that early embryo defects in selfed *wei8 tar1* plants might be caused by compromised auxin biosynthesis in maternal tissues rather than in the embryo itself. To test this notion, we analysed early embryo development in reciprocal crosses between wild type and *wei8 tar1* (Fig. 3b). When *wei8 tar1* ovules were fertilized with wild-type pollen, but not in the reverse cross, we observed defective embryo phenotypes indistinguishable from the ones in selfed *wei8 tar1* controls. We conclude that with regard to early embryogenesis, *wei8* and *tar1* are maternal effect mutations. Furthermore, pollinating double heterozygous *wei8/+ tar1/+* plants with wild-type pollen resulted in normal developing embryos, suggesting that the maternal sporophytic tissue, such as the integuments, rather than the female gametophyte is responsible (Fig. 3b). We confirmed this finding by expressing the bacterial *IAA-lysine synthetase* (*iaaL*), which inactivates free auxin through conjugation<sup>19</sup>, specifically in the integuments using the *BANYULS* (*BAN*) promoter<sup>20</sup>. *pBAN::iaaL* expression causes a strong reduction of *pDR5:GFP* signal in this region after pollination with no detectable expression in the embryo attachment region (Fig. 3c-d and Supplementary Table 2) and results in defective embryo development similar to selfed *wei8 tar1* controls (Fig. 3a). Reciprocal crosses confirm that *pBAN::iaaL* affects embryo development only when provided through the mother (Fig. 3b). Together, these observations provide evidence that maternal auxin production in the integuments contributes to early embryo development.

The incomplete penetrance of recognizable early embryo defects with a compromised maternal IPyA pathway suggests the existence of functionally redundant and compensatory mechanisms. For example, a recent study revealed that auxin synthesized in the developing endosperm is transported into the integuments, where it promotes development of the seed coat<sup>21,22</sup>. Because endosperm development initiates before the first division of the zygote, endosperm-produced auxin could also contribute to early embryo development, either directly or via the integuments. Our reciprocal crosses, however, do not suggest a prominent role of endosperm-derived auxin in early embryogenesis.

Notably, similar embryo defects to those caused by the absence of maternal auxin production have been described for zygotic mutations affecting auxin transport from the

suspensor to the embryo<sup>9,23,24</sup> or auxin response within the embryo<sup>8</sup>. Therefore, we considered two hypotheses to explain the requirement of auxin biosynthesis in the integuments for embryo development. First, an auxin response in the integuments could cause the production of a downstream signal to the embryo, influencing its development. To address this hypothesis, we expressed an auxin-insensitive version of *BODENLOS/AUX-IAA12 (BDL)*, a broad repressor of the transcriptional auxin response<sup>25</sup>, from the *pBAN* promoter. *pBAN:bdl* expression strongly reduces *pDR5:GFP* auxin response in the integuments (Fig. 3e and Supplementary Table 2). Nonetheless, this does not result in any observable embryo defects (Fig. 3a) suggesting that BDL-mediated auxin response and downstream processes in the integuments do not play a major role for embryo development.

An alternative hypothesis holds that the integuments provide auxin directly to the embryo. Consistent with this idea and a recent report<sup>26</sup>, we find that several auxin transport facilitators (PINs, AUX1, LAX1, ABCB1 and ABCB19) are expressed in the integuments (Supplementary Fig. 6). Of the facilitators tested, only AUX1 and LAX1 could be involved in the auxin flow between micropyle cells and early embryo based on their expression and intracellular localization. However, multiple mutants did not reveal any sporophytic maternal-dependent embryo phenotypes, possibly due to genetic redundancy, or confounding gametophytic defects as in *aux1* mutants (not shown). We therefore analysed whether auxin production in the embryo might complement the maternal auxin defects to test our second hypothesis. To this end, we expressed the bacterial auxin biosynthetic enzyme *iaaM27* from the *WOX2* promoter throughout embryos of *wei8 tar1* plants. We found that the embryo defects in *wei8 tar1* mutants are significantly suppressed by the *pWOX2:iaaM* transgene (Fig. 3a), suggesting that ectopic auxin production in the embryo can overcome the reduction of maternal auxin supply.

This study provides insight into the mechanisms of how the mother plant contributes to the regulation of early embryogenesis. A straightforward interpretation of our results is that maternal auxin contributes to the reported auxin accumulation in the apical proembryo where it mediates early embryo development<sup>9</sup>. Supporting to this notion are predictions from recent mathematical modeling and experimental results showing that a local auxin source coupled to feedback regulation of PIN polarity<sup>28,29</sup> in the embryo is sufficient to generate a robust auxin gradient that instructs apical-basal axis formation<sup>10,28</sup>. Although, we cannot exclude that auxin synthesized in the maternal integuments generates an additional, unknown downstream signal that affects embryogenesis, the observation that auxin-mediated transcriptional output in these tissues is not required for regulating embryogenesis did not provide evidence for this alternative model. Together with recent reports<sup>21,22,26</sup>, our data contribute to understanding auxin dynamics during development of the three compartments of the ovule; the integument, the endosperm, and the embryo: Before fertilization, stamen maturation restricts auxin export from the ovule<sup>26</sup>. Subsequently, fertilization causes further restriction of auxin export through the funiculus, resulting in the spread of auxin throughout the integuments<sup>26</sup>. The data presented here reveal that expression of the key biosynthetic enzyme TAA1 gradually increases in the integuments. Pollination then triggers a strong upregulation of local auxin accumulation in the integuments, which affect early steps in embryo development. Because fertilization has usually taken place at 24 hours after fertilization, future experiments will address which step

during pollination and/or fertilization triggers these events. Finally, fertilization-induced auxin production in the endosperm signals back to the integuments, regulating seed coat development<sup>21,22</sup>. Thus, a circuitry of localized auxin accumulation, signaling, and activity coordinates embryo, endosperm and seed coat development.

## Materials and Methods

### Plant material, growth conditions and plant treatment

For all experiments, *Arabidopsis* plants were grown in long-day (16 h light/8 h dark) conditions at 18–20°C. The plant lines used in this study are listed in supplements. MG132 treatment was done on ovules at 24 HAP by incubation in liquid MS supplemented with 50 µM MG132 (Sigma-Aldrich, stock dissolved in DMSO) for 6 h. For backcrosses experiments, embryo development was analysed between 2 to 5 days after pollination. Embryos were counted as defective when the apical cell division diverged from the wild-type vertical division or the size of the apical cells or suspensor was affected. Genotypes of parental plants were confirmed by PCR. Hand pollination was done by emasculating the biggest unopened bud from the main shoot and by pollinating the stigma either immediately or after 24 h. For the experiment, *R2D2* plants were selected by fluorescence in the main root tip.

### Cloning

Coding sequences of *iaaL* and *bdI* were amplified (primer sequences in Supplementary Table 3) from *pSDM7012* and *pIC-myc-bdI* and inserted into a blunted NcoI site of *pBAN-pBS-SK*. Using Sall site of *pBAN-pBS-SK*, *pBAN:iaaL* and *pBAN:bdI* are transferred after blunting into a SmaI site of a binary vector (*pGIK*). Coding sequence of *iaaM* was amplified (primer sequences in Supplementary Table 3) from *pSDM7010* and inserted into a blunted Sall site of a binary vector containing *WOX2* promoter sequence (ZJ62). Constructs were transformed into *Arabidopsis* wild type by floral dip. *pBAN:iaaL* and *pBAN:bdI* lines are kanamycin resistant. *pWOX2:iaaM* line is MTX resistant.

### Auxin response in maize ovules

Maize *pDR5:mRFP* plants<sup>30</sup> were grown under standard greenhouse conditions with 16 h light at 26°C and 8 h darkness at 22°C and a relative air humidity of 40 to 60%. Cobs were covered before ovule maturation and hand-pollinated when the silks reached a length of 2–3 cm outside the cobs. About 50% of silks were pollinated with fresh pollen (limited pollination). Before pollination as well as 2–5 days after pollination (DAP) ovules were longitudinally sectioned by hand along the embryo sac axis. Samples were mounted in 13% mannitol (w/v) solution on glass slides under a coverslip. Imaging was done using a Leica SP8 inverted confocal laser scanning microscope at 561 nm with a 570–666 nm band-pass emission filter.

### Microscopy

For embryo phenotyping, embryos were cleared at mentioned stages in a chloral hydrate solution (chloral hydrate/water/glycerol, 8/3/1, w/v/v). Microscopy observations were done on a Zeiss Axioskop2 plus coupled to an AxioCam MRc camera, or an Olympus BX51

microscope, coupled to a Sony DS-5M-L1 camera, using differential interference contrast optics. For fluorescent visualization, ovules were mounted in 10% glycerol or 7% glucose with or without 0.1 mg/mL propidium iodide. Imaging was done on a Zeiss Axio Imager A1 coupled to an AxioCam MRm camera (wide-field fluorescence) or on a Zeiss LSM 700 or a ZEISS LSM 780 based on Zeiss Axio Observer Z1 microscopes, and a Zeiss LSM 700 based on a Zeiss Axio Imager Z2 microscope (confocal fluorescence). Acquisition with multiple channels was done by sequential scanning using 488 nm (GFP, YFP, propidium iodide) and 550 nm (TdTomato) with 505-530nm band pass (GFP, YFP) and 530-600 band pass (propidium iodide, TdTomato) emission filters.

### Fluorescence signal quantification

We used wide-field fluorescence microscopy (see above) to quantify the expression pattern of fluorescent markers in the embryo attachment region in ovules of *pTAA1:GFP-TAA1*, *pDR5:GFP* and *R2D2* plants. Flowers at stage 12c of *pTAA1:GFP-TAA1*, *pDR5:GFP* and *R2D2* lines were emasculated 24 h before hand pollination. Respective pistils were pollinated with either *pTAA1:GFP-TAA1*, *pDR5:GFP* or *R2D2* pollen. Pistils were collected at 0 h after emasculation (0 HAE), 0 h after pollination (0 HAP, equivalent to 24 HAE) and 24 HAP. Representative microscopic pictures are displayed in Supplementary Fig. 2. Unpollinated pistil (UNP) corresponding to a 48 HAE is used as control. From self pollinating flowers, ovules were collected one day before flowering (DBF), at flowering day (FD) and one, two, three or four days after flowering (DAF). In our conditions, FD corresponds to approximately 0 HAP of hand-pollinated ovules (four-celled female gametophyte), 1 DAF to approximately 12 HAP-24 HAP (1 to 8 nucleated endosperm and zygote), and 2 DAF to approximately 24 HAP-30 HAP (>8 nuclei in endosperm and zygote to one-cell embryo). Ovules were mounted in 10% glycerol for fluorescent visualization and quantification. For the quantification of GFP signal in *pTAA:GFP-TAA1* and *pDR5:GFP* lines, we integrated the brightness of GFP multiplying the area with the pixels, and for *R2D2* line we measured the n3xVENUS and ntdTomato pixels and calculated the mDII/DII ratio; the quantifications were done using AxioVisionLE 4.7.1.0 (Carl Zeiss Imaging Solutions GmbH). Presented data are means  $\pm$  s.e.m, overlaid by the corresponding dot plots. Kruskal-Wallis Test (Nonparametric ANOVA) with Dunn's Multiple Comparisons Test was performed for all samples using GraphPad InStat 3.1 software, with the exception of Fig 3a-b using R version 3.4.5 (The R foundation for Statistical Computing). The presented data in Fig. 1 are normalized to the value for 0 HAP (hand pollination) or FD (self pollination). The graphs were prepared using GraphPad Prism software.

### Auxin quantification

OxIAA levels were found to mirror auxin levels also in other tissues. It is an inactivate auxin molecule, the main production of auxin catabolism, and has no biological activity<sup>31</sup>. IAAsp is a conjugated product of the Asp amino acid of IAA. It is a reversible product of a GH3-dependent catabolic pathway used to balanced the levels of active IAA<sup>31</sup>. IAA and metabolites were quantified in four samples, including two genotypes (Col and *wei8 tar1*) and two time points (0 HAP [24 h after emasculation of unpollinated gynoecea] and 24 HAP [24 h after hand pollination of emasculated gynoecea]). Six-week old plants were grown in soil in controlled environment (PSI Fytoscope FS-WI, long-day regime with LED

illumination, 21°C, 50% humidity). For each sample approximately 750 ovules were collected for each biological replicate, in five biological replicates. The exact number of siliques from which the ovules were collected, and the exact number of collected ovules per replicate are indicated in Supplementary Table 1. Ovules collection of one sample replicate took approx. 90 minutes. Collection was performed under a dissection microscope (SZ51 Olympus). A gynoeceium was harvested from a plant and stuck on double-sided tape. Using a 30G hypodermic needle (Terumo) the gynoeceium was cut along the septum and the carpel stuck to the tape. Using Dumont #5 tweezers ovules were harvested and collected into a 1.5 ml tube on dry ice. While collecting the exact number of ovules were counted using a manual cell counter.

Extraction and purification were performed following the procedure as described<sup>32</sup>. 5 pmol of [<sup>13</sup>C<sub>6</sub>]IAA, [<sup>13</sup>C<sub>6</sub>]oxIAA and [<sup>13</sup>C<sub>6</sub>]IAA<sub>sp</sub> were added to each sample as an internal standards. IAA and IAA metabolites were quantified by LC-MS/MS method<sup>32</sup>. All data were processed using MassLynx™ software (ver. 4.1, Waters).

## Statistics and Reproducibility

Fig 1a: Similar result was observed in around 1000 ovules in more than 50 plants by two experimenters.

Fig. 1b and Supplementary Table 1 (data source): The observations were independently repeated twice with similar output. Plotted data are the means of 5 replicates presented as pmol/1000 ovules, ± s.d. The exact number of ovules for each sample is indicated in Supplementary Table 1. Significant differences between 24 HAP wild-type ovules and either 0 HAP wild-type ovules, 0 HAP *wei8 tar1* ovules or 24 HAP *wei8 tar1* ovules were determined by two-way ANOVA followed by Tukey's multiple comparison test (\*\*\*\*p<0.0001) with a two-sided 95 % confidence interval of difference.

Fig. 1c-1d: Similar result was observed in around 200 ovules in more than 10 plants by two experimenters.

Fig. 1e-1f: The observations were independently repeated twice with similar results. Data represent individual points with means at horizontal bars ± s.e.m at vertical bars. Significance of differences was determined by Kruskal-Wallis Test (Nonparametric ANOVA) with Dunn's Multiple Comparisons Test: \*\*\*p < 0.001; \*\*p < 0. 01; \*p < 0. 05; n.s., not significant, with a two-sided 99.9 % confidence interval. In (e), n = 96 (R2D2), 120 (DR5), 180 (TAA1 – 0 HAE, 0 HAP, 24 HAP), 179 (TAA1 – UNP) biologically independent ovules. In (f), n = 49 (R2D2 – 1 DBF), 37 (R2D2 - FD), 20 (R2D2 – 1 DAF), 50 (R2D2 – 2 DAF), 48 (DR5), 50 (DR5 – 1 DBF), 51 (DR5 - FD), 48 (DR5 – 1 DAF), 51 (DR5 – 2 DAF) biologically independent ovules. Representative pictures are in Supplementary Fig. 2.

Fig. 2a-2d: Similar result was observed twice by two experimenters.

Fig. 3a-b: NA, test not applicable; p-values by two-sided Fisher's exact test compared to wild type, except for *pWOX2:iaaM wei8 tar1* that was compared to *wei8 tar1* in (a) and compared to the respective reciprocal crosses in (b).



Fig. 2e, Fig. 3a-b, Supplementary Fig. 5: The observations were independently repeated more than 3 times with similar results in 3 different laboratories (Freiburg, Ghent, Brno), except for the data on *wei8-3* and *wei8-11* alleles repeated twice.

Fig. 3c-3e, Supplementary Figs 4, 6: The observations were repeated independently three times with similar results.

Supplementary Fig. 1: The observations were independently repeated twice with similar results

Supplementary Fig. 3: The similar results were independently observed on 10 independent biological samples.

## Supplementary Material

Refer to Web version on PubMed Central for supplementary material.

## Acknowledgements

We thank Edwin Groot for assistance with statistical analyses and for critical reading of the manuscript. We thank J. Alonso for providing *wei8-1*, *wei8-1 tar1-1*, *pDR5:GFP wei8-1*, and *pTAA1:GFP-TAA1* seeds, G. Jürgens for providing *pDR5:nls-3xGFP* and *pDR5:nls-3xGFP wei8-1 tar1-1* seeds, T. Vernoux for *p35S:DII-VENUS* and *p35S:mDII-VENUS* seeds and plasmids, R. Offringa for *pSDM7010* and *pSDM7012*, L. Lepiniec for *pBAN-pBS-SK*, Che-Yang Liao and Dolf Weijers for *R2D2* seeds, and Thomas Friedrich for valuable suggestions. Seeds of *wei8-3* and *wei-11* seeds were obtained from the European *Arabidopsis* Stock Center (NASC). We acknowledge the CEITEC core facility CELLIM supported by the MEYS CR (LM2015062 Czech-BioImaging), and the CEITEC core facility Plant Sciences.

### Funding

H.S.R. was supported by the SoMoProII program co-financed by the South-Moravian Region and the European Union, by the Ministry of Education, Youth and Sports of the Czech Republic within CEITEC 2020 (LQ1601) and by the Masaryk University.

C.P. was supported by the Kwanjeong Educational Foundation.

C.L.G. was supported by the Deutscher Akademischer Austauschdienst.

W.G. was a post-doctoral fellow of the Research Foundation Flanders.

B.W. was supported by the “NITKA” project under European Social Fund UDA-POKL.04.03.00-00-168/12, realized in the University of Silesia, Katowice, Poland.

A.P and O.N. were supported by the Czech Foundation Agency (GA17-21581Y) and the Ministry of Education, Youth and Sports of the Czech Republic via the National Program for Sustainability (LO1204).

J.C. is a post-doctoral fellow supported by a grant from the Deutsche Forschungsgemeinschaft (Dr334/10) to T.D.

This work was further supported by the European Research Council (FP7/2007-2013 / ERC-grant agreement n° 282300 to J.F.), and the Czech Science Foundation GACR (GA13-40637S) to J.F.; and by the Deutsche Forschungsgemeinschaft (La606/6, La606/13, La606/17 and ERA-CAPS program), and the EU 7<sup>th</sup> framework program (ITN SIREN) to T.L.

This material reflects only the author's views and the European Union is not liable for any use that may be made of the information contained therein.

## References

1. Figueiredo DD, Köhler CC. Auxin: a molecular trigger of seed development. *Genes Dev.* 2018; 32:479–490. [PubMed: 29692356]
2. Mansfield SG, Briarty LG. Early embryogenesis in *Arabidopsis thaliana* 2. the developing embryo. *Canadian Journal of Botany-Revue Canadienne De Botanique.* 1991; 69:461–476.
3. Johnstone O, Lasko P. Translational regulation and RNA localization in *Drosophila* oocytes and embryos. *Annu Rev Genet.* 2001; 35:365–406. [PubMed: 11700288]
4. Riechmann V, Ephrussi A. Axis formation during *Drosophila* oogenesis. *Curr Opin Gen Dev.* 2001; 11:374–383.
5. Ray S, Golden T, Ray A. Maternal effects of the *short integument* mutation on embryo development in *Arabidopsis*. *Dev Biol.* 1995; 180:365–369.
6. Prigge MJ, Wagner DR. The *Arabidopsis* *SERRATE* gene encodes a zinc-finger protein required for normal shoot development. *Plant Cell.* 2001; 13:1263–1280. [PubMed: 11402159]
7. Costa LM, et al. Central cell-derived peptides regulate early embryo patterning in flowering plants. *Science.* 2014; 344:168–172. [PubMed: 24723605]
8. Möller BK, Weijers D. Auxin control of embryo patterning. *Cold Spring Harbor Perspect Biol.* 2009; 1:a001545.
9. Friml J, et al. Efflux-dependent auxin gradients establish the apical-basal axis of *Arabidopsis*. *Nature.* 2003; 426:147–153. [PubMed: 14614497]
10. Robert HS, et al. Local auxin sources orient the apical-basal axis in *Arabidopsis* embryos. *Curr Biol.* 2013; 23:2506–2512. [PubMed: 24291089]
11. Brunoud G, et al. A novel sensor to map auxin response and distribution at high spatio-temporal resolution. *Nature.* 2012; 482:103–106. [PubMed: 22246322]
12. Liao C-Y, et al. Reporters for sensitive and quantitative measurement of auxin response. *Nat Methods.* 2015; 12:207–210. [PubMed: 25643149]
13. Paciorek T, Friml J. Auxin signaling. *Journal of Cell Science.* 2006; 119:1199–1202. [PubMed: 16554435]
14. Ljung K. Auxin metabolism and homeostasis during plant development. *Development.* 2013; 140:943–950. [PubMed: 23404103]
15. Stepanova AN, et al. The *Arabidopsis* YUCCA1 flavin monooxygenase functions in the indole-3-pyruvic acid branch of auxin biosynthesis. *Plant Cell.* 2011; 23:3961–3973. [PubMed: 22108406]
16. Mashiguchi K, et al. The main auxin biosynthesis pathway in *Arabidopsis*. *Proc Natl Acad Sci USA.* 2011; 108:18512–18517. [PubMed: 22025724]
17. Won C, et al. Conversion of tryptophan to indole-3-acetic acid by TRYPTOPHAN AMINOTRANSFERASES OF ARABIDOPSIS and YUCCAs in *Arabidopsis*. *Proc Natl Acad Sci USA.* 2011; 108:18518–18523. [PubMed: 22025721]
18. Stepanova AN, et al. TAA1-mediated auxin biosynthesis is essential for hormone crosstalk and plant development. *Cell.* 2008; 133:177–191. [PubMed: 18394997]
19. Jensen PJ, Hangarter RP, Estelle M. Auxin transport is required for hypocotyl elongation in light-grown but not dark-grown *Arabidopsis*. *Plant Physiol.* 1998; 116:455–462. [PubMed: 9489005]
20. Debeaujon I, et al. Proanthocyanidin-accumulating cells in *Arabidopsis* testa: regulation of differentiation and role in seed development. *Plant Cell.* 2003; 15:2514–2531. [PubMed: 14555692]
21. Figueiredo DD, Batista RA, Roszak PJ, Köhler CC. Auxin production couples endosperm development to fertilization. *Nature Plants.* 2015; 15184. doi: 10.1038/nplants.2015.184
22. Figueiredo DD, Batista RA, Roszak PJ, Hennig L, Köhler CC. Auxin production in the endosperm drives seed coat development in *Arabidopsis*. *eLife.* 2016; 5:e20542. [PubMed: 27848912]
23. Blilou I, et al. The PIN auxin efflux facilitator network controls growth and patterning in *Arabidopsis* roots. *Nature.* 2005; 433:39–44. [PubMed: 15635403]
24. Vieten A, et al. Functional redundancy of PIN proteins is accompanied by auxin-dependent cross-regulation of PIN expression. *Development.* 2005; 132:4521–4531. [PubMed: 16192309]

25. Weijers D, et al. Auxin triggers transient local signaling for cell specification in Arabidopsis embryogenesis. *Dev Cell*. 2006; 10:265–270. [PubMed: 16459305]
26. Larsson E, Vivian-Smith A, Offringa R, Sundberg E. Auxin homeostasis in Arabidopsis ovules Is anther-dependent at maturation and changes dynamically upon fertilization. *Front Plant Sci*. 2017; 8:315–14. [PubMed: 28337213]
27. Weijers D, et al. Maintenance of embryonic auxin distribution for apical-basal patterning by PIN-FORMED-dependent auxin transport in Arabidopsis. *Plant Cell*. 2005; 17:2517–2526. [PubMed: 16055631]
28. Wabnik K, Robert HS, Smith RS, Friml J. Modeling framework for the establishment of the apical-basal embryonic axis in plants. *Curr. Biol*. 2013; 23:2513–2518. [PubMed: 24291090]
29. Prat T, et al. WRKY23 is a component of the transcriptional network mediating auxin feedback on PIN polarity. *PLoS Genet*. 2018; 14:e1007177. [PubMed: 29377885]
30. Gallavotti A, Yang Y, Schmidt RJ, Jackson DP. The relationship between auxin transport and maize branching. *Plant Physiol*. 2008; 147:1913–1923. [PubMed: 18550681]
31. Zhang J, Peer WA. Auxin homeostasis: the DAO of catabolism. *J Exp Bot*. 2017; :1–10. DOI: 10.1093/jxb/erx221
32. Pencík A, et al. Ultra-rapid auxin metabolite profiling for high-throughput mutant screening in Arabidopsis. *J Exp Bot*. 2018; 69:2569–2579. [PubMed: 29514302]

### Impact statement

Early embryo development requires auxin production in the surrounding maternal integuments.

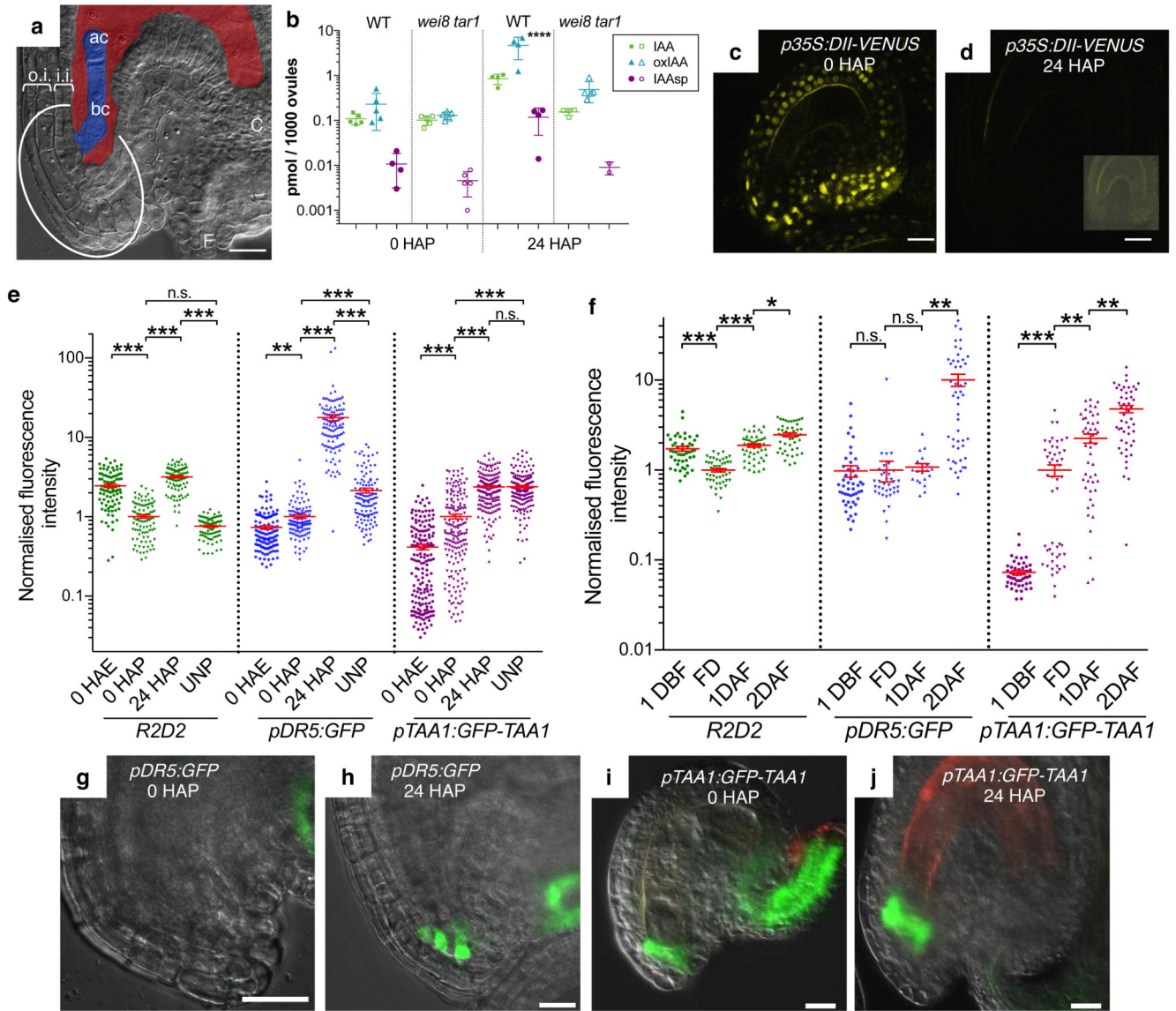


**Fig. 1. Auxin accumulation in integuments.**

**a**, Micropylar region of an *Arabidopsis* fertilized seed. Embryo and endosperm are colored in blue and red, respectively. ac, apical cell; bc, basal cell; C, chalaza; F, funiculus; o.i., outer integument; i.i., inner integument; the embryo attachment region is circled. **b**, Quantification of IAA, IAA-Aspartate (IAAsp), and oxidized IAA (oxIAA) in wild-type (WT) and *wei8 tar1* ovules. **c-d**, *p35S:DII-VENUS* expression (yellow signal) in unfertilized (**c**) and 24 HAP (**d**) ovules. Inset in (**d**) shows the same ovule with enhanced brightness. **e-f**, Quantification in the embryo attachment region of GFP fluorescence (*pDR5:GFP* and *pTAA1:GFP-TAA1*) and mDII/DII ratio, normalized to 0 HAP (**e**) and FD (**f**). Data presented as individual points with a horizontal bar at the mean  $\pm$  s.e.m at the vertical bar. **g-j**, *pDR5:GFP* and *pTAA1:GFP-TAA1* expression in the wild-type embryo attachment region. Green GFP signal, merged with the brightfield image. Reddish signal, autofluorescence. Scale bars, 20  $\mu$ m.

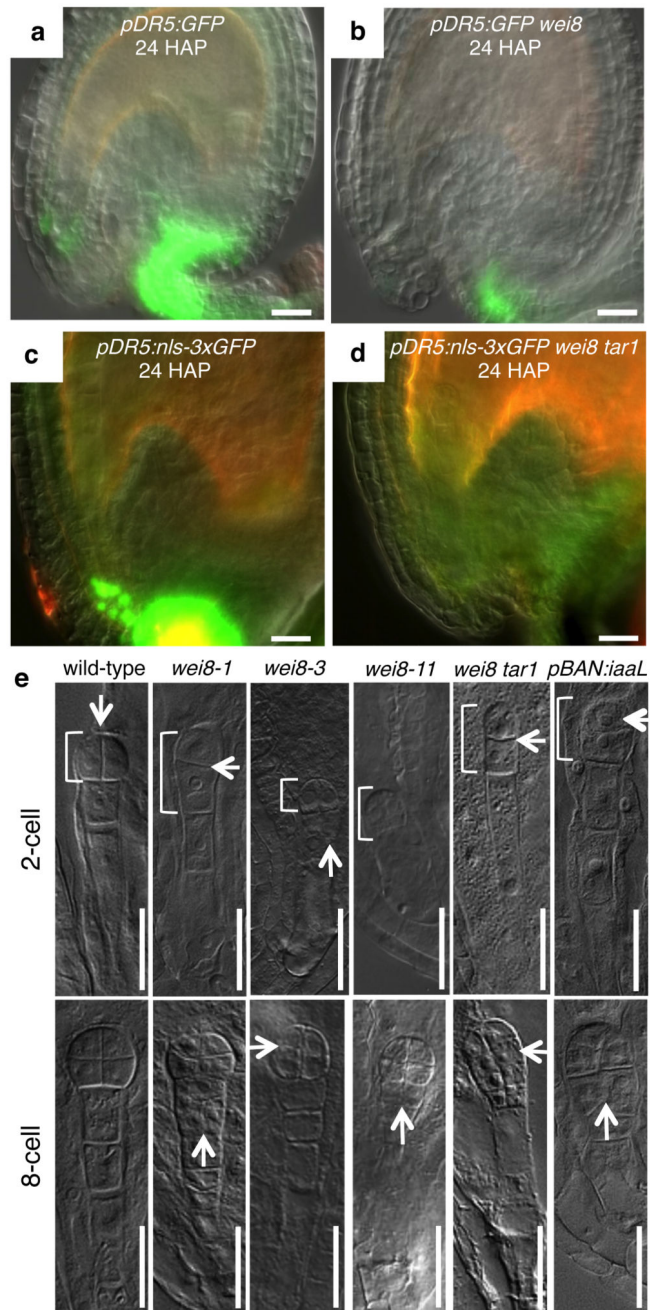


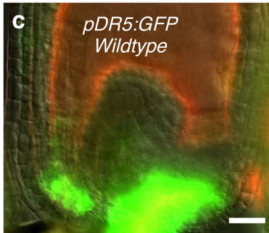
**Fig. 2. Auxin biosynthesis mutants display early embryonic defects.**  
**a-d**, *pDR5:GFP* expression from indicated genotypes. Green GFP signal, merged with brightfield images. Autofluorescence appears reddish. **e**, Two- and eight-cell embryo phenotypes from indicated genotypes. Arrows, abnormal division planes. Brackets mark proembryos. Scale bars, 20 μm.

a		Genotype of mother plant		n	Percentage of defective embryos	
		wild type		563	0.36	
		<i>wei8</i>		463	12.75	****
		<i>wei8 tar1</i>		435	18.58	****
		<i>pBAN:iaaL #1</i>		395	14.68	****
		<i>pBAN:iaaL #7</i>		386	18.91	****
		<i>pBAN:bdl #2</i>		174	0.00	n. s.
		<i>pBAN:bdl #3</i>		170	0.00	n. s.
		<i>pWOX2:iaaM wei8 tar1 #2</i>		307	2.93	****
		<i>pWOX2:iaaM wei8 tar1 #3</i>		365	3.01	****

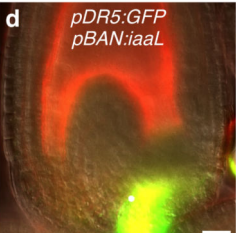
  

b			Parental genotypes		n	Percentage of defective embryos	
♀	×	♂					
wild type	×	<i>wei8 tar1</i>		146	0.00		
<i>wei8 tar1</i>	×	wild type		633	14.70	****	
<i>wei8/+ tar1/+</i>	×	wild type		133	0.00	n.s.	
wild type	×	<i>pBAN:iaaL #1</i>		169	0.59		
<i>pBAN:iaaL #1</i>	×	wild type		298	11.41	****	
wild type	×	<i>pBAN:iaaL #7</i>		192	0.00		
<i>pBAN:iaaL #7</i>	×	wild type		334	14.07	****	
wild type	×	wild type		270	4.07		
<i>wei8-1</i>	×	wild type		507	17.56	****	
<i>wei8-3</i>	×	wild type		386	22.80	****	
<i>wei8-11</i>	×	wild type		437	25.17	****	

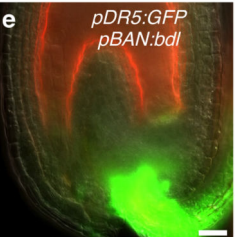
  



**c** *pDR5:GFP*  
Wildtype



**d** *pDR5:GFP*  
*pBAN:iaaL*



**e** *pDR5:GFP*  
*pBAN:bdl*

**Fig. 3. Sporophytic maternal early embryonic defects.**

**a-b**, Frequencies of the embryo phenotypes in self-fertilized plants (**a**) and reciprocal crosses (**b**) of indicated genotypes. NA, not applicable; p-values by two-sided Fisher's exact test compared to wild type, except for *pWOX2:iaaM wei8 tar1* that was compared to *wei8 tar1* in (**a**) and compared to the respective reciprocal crosses in (**b**). **c-e**, *pDR5:GFP* expression (green) at 24 HAP from indicated genotypes. Autofluorescence is reddish. Scale bars, 20µm.